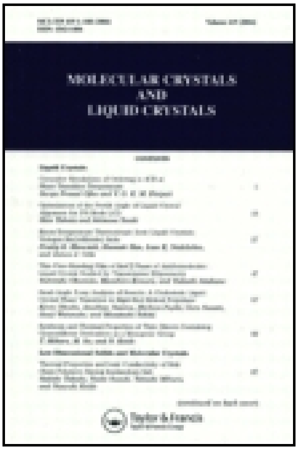

Molecular Crystals and Liquid Crystals
Publication details, including instructions for authors and subscription information:
http://www.tandfonline.com/loi/gmcl20

Comparing Liquid Crystalline Properties of Two Epoxy Compounds Based on the Same Azoxy Group

B. Mossety-Leszczak [a] , M. Wlodarska [b] , H. Galina [a] & G. W. Bak [b]
[a] Department of Industrial and Materials Chemistry, Rzeszow University of Technology, Rzeszow, Poland
[b] Institute of Physics, Technical University of Lodz, Lodz, Poland

Version of record first published: 22 Sep 2010

To cite this article: B. Mossety-Leszczak, M. Wlodarska, H. Galina & G. W. Bak (2008): Comparing Liquid Crystalline Properties of Two Epoxy Compounds Based on the Same Azoxy Group, Molecular Crystals and Liquid Crystals, 490:1, 52-66

To link to this article: http://dx.doi.org/10.1080/15421400802305830

Mol. Cryst. Liq. Cryst., Vol. 490, pp. 52–66, 2008
Copyright © Taylor & Francis Group, LLC
ISSN: 1542-1406 print/1563-5287 online
DOI: 10.1080/15421400802305830

Comparing Liquid Crystalline Properties of Two Epoxy Compounds Based on the Same Azoxy Group

B. Mossety-Leszczak[1], M. Wlodarska[2], H. Galina[1], and G. W. Bak[2]
[1]Department of Industrial and Materials Chemistry, Rzeszow University of Technology, Rzeszow, Poland
[2]Institute of Physics, Technical University of Lodz, Lodz, Poland

Two recently synthesised diepoxy compounds based on the same rigid central segment with carbon chains of different lengths were compared. Microscopic observations, differential scanning calorimetry (DSC) and dielectric measurements confirmed the existence of a mesophase in both compounds and enabled determination of the temperatures of phase transitions. Wide-angle X-ray scattering (WAXS) measurements and optical observations enabled identification of mesophase types. Nematic phase appeared in both compounds; in the material with longer chains smectic A phase was also detected. Lengths of the molecules and average nearest neighbor distances were estimated using the wide-angle X-ray scattering results. Lengths of the molecules were also computed by quantum mechanical methods resulting in very good agreement with the experimental data.

Keywords: epoxy resins; liquid crystals; phase transition

1. INTRODUCTION

Despite more than 30 years of history of liquid crystalline (LC) displays there is a continuous interest in liquid crystal materials [1]. It stems from the enormous range of applications where liquid crystals are utilized for their ability to change their optical properties quickly in response to various electric or magnetic fields, temperature gradients, *etc.* [2]. Nowadays, besides LC monomers there are many other types of liquid crystal materials (*e.g.*, columnar, discotic, main and

---

Address correspondence to M. Wlodarska, Institute of Physics, Technical University of Lodz, 90-924 Lodz, Poland. E-mail: magdaw@p.lodz.pl

side chain polymers, elastomers) which find new applications in the industry [3–5]. In any innovative LC device, novel components and materials play important roles [1].

The epoxy compounds are now commercially used as reagents for curing because the obtained products of curing have very good mechanical properties. Thanks to the lack of side products during processing, small contraction, and high liquidity, they can be used to make thin-walled and complex moldings [6]. LC epoxy compounds can also be used to build larger structures known as LC polymer networks. Such epoxy precursors with different mesogenic groups have been synthesized and characterized by several scientific groups [5,7,8]. LC properties of a resin change the physical properties of the resultant polymer network because of additional ordering of molecules present both during the reaction and in the cured product. As an example, excellent transparency and high birefringence of these networks can be achieved by polymerization of LC monomers in unidirectional orientation [9]. We also attempt to use the LC monomers for curing, but to control this process and the properties of cured materials, knowledge about the properties of pure monomers is essential [10].

The aim of this article is to compare basic physical properties of two new diepoxy materials with different carbon chains. The synthesis route is presented along with the results of optical, dielectric, and differential scanning calorimetry measurements, which allowed for precise determination of phase transitions. WXAS measurements confirmed the type of the mesophase. Approximate lengths of the molecules and average distances between them were also obtained in these investigations. The molecular lengths were compared to the values computed theoretically with the use of *ab initio* methods [11,12].

2. MATERIALS

We synthesised two diepoxy compounds based on the same core but differing in the length of the carbon chains. Their molecular structures are shown in Fig. 1.

Investigations using *ab initio* methods [12] resulted in establishing the geometry of the molecules. The calculations were carried out for a single molecule, without taking into account any interactions with other molecules or the surrounding medium. Lengths of the molecules were estimated as distances between two outermost atoms. As the studied structures are linear and the terminal atoms are hydrogens, this approximation should not introduce a significant error.

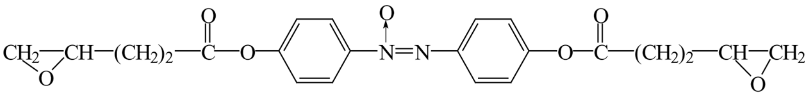

compound 1 (**4a**)

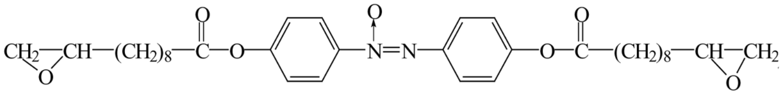

compound 2 (**4b**)

FIGURE 1 Molecular structure of the investigated compounds.

Geometry optimization was performed following a two-step method proposed in the article [12] for similar monomers, where details of the procedure can be found. In the first step, the investigated structures were split into three segments: the rigid core and two chains, which were optimized as if they were separate molecules. Subsequently, original molecules were reconstructed from the optimized segments (taking into account several possible orientations of the chains with respect to the central segment) and underwent final energy minimization. Following the article [13], where the geometry of a similar molecule (PAA) was analyzed, we assumed that the azoxy group of the central segment is coplanar with the aromatic rings. For both the investigated molecules the calculations revealed two stable conformations differing in mutual orientation of the C=O groups. Both conformations in either pair have very similar values of energy, which means that they are likely to coexist in real materials. Length of the molecule is also almost the same in both isomers, despite the structural differences.

3. EXPERIMENTAL

All starting materials were commercial reagents (Aldrich, Fluka, Merck) and were used without further purification. The chemical structure of products was confirmed by ^{1}H-NMR and FTIR spectroscopy, by using a Bruker Avance^{II} 500 and a Paragon 1000 FT-IR spectrometer, respectively. The purity of epoxy compounds was assessed chemically by titration its chloroform solution containing tetraethylammonium bromide with perchloric acid solution in anhydrous acetic acid. The procedure described in the standard ISO 3001–1978 was used. The thus measured epoxy numbers (in moles of epoxy groups per 100 g) differed from calculated ones by less than 1%.

The textures of the compounds were observed using a polarising microscope Zeiss at a magnification of 80×. The temperature was controlled by means of a Linkam TMS 91 hot stage. The measurements were carried out in cells of two kinds, one composed of parallel glass plates covered with conducting layers and the others in which the electrodes were also covered with thin polyimide film with anti-parallel rubbing. This additional coating enforced planar orientation of LC samples. The sample thickness was $5 * 10^{-6}$ m in the cell with polyimide layer.

DSC measurements were performed with the use of a Mettler Toledo DSC822^{e} instrument under nitrogen atmosphere. The thermograms recorded at heating and cooling rate of 2 deg/min allowed for determination of phase transitions.

WAXS measurements were conducted using a rotating anode (Rigaku 18 kW) X-ray beam with a pinhole collimation and a two-dimensional detector (Siemens) with 1024 × 1024 pixels. A double graphite monochromator for the CuK_{α} radiation ($\lambda = 0.154$ nm) was used. The beam diameter was about 0.5 mm and the sample to detector distance was 80 mm. Measurements were performed in various temperatures for samples molten in glass capillaries.

Temperature-dependent dielectric measurements were performed using the experimental set-up of Novocontrol. The system was equipped with Alpha high-resolution dielectric analyzer, Quatro v.4.0 temperature controller. The AC voltage applied to the capacitor was 0.5 V, and the frequency for the static dielectric constant was 10 kHz, the samples were in sandwich-type cells. The temperature was controlled using a nitrogen-gas cryostat and the temperature stability of the sample was better than 0.1 K.

Ab initio calculations were conducted using restricted Hartree–Fock (RHF) method with the standard 6–31G* basis set. The structures of all molecules were optimised to a minimum of energy using Berny algorithm [14]. The optimization procedure was described in detail (for other, but similar materials) in [12]. All the computations were carried out using *Gaussian 03* program suite [11] running on a PC workstation.

4. RESULTS AND DISCUSSION

4.1. Synthesis

4.1.1. Synthesis of 4,4′-Dihydroxyazobenzene

The synthesized epoxy compounds were derivatives of 4,4′-dihydroxyazobenzene (**1**). The synthesis of 4,4′-dihydroxyazobenzene was earlier described in literature [15,16]. In this work, we use the way similar to the method described by P. Vanoppen *et al.* [15]. 4,4′-dihydroxyazobenzene was obtained by azo coupling of diazonium salt of 4-hydroxyaniline with phenol dissolved in solution of sodium hydroxide.

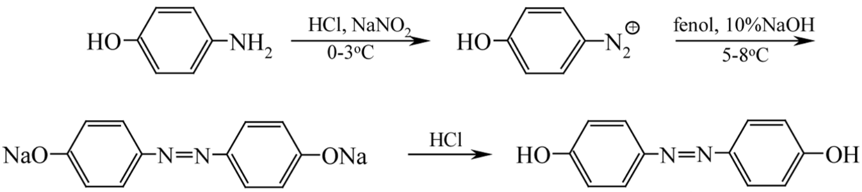

1

4-hydroxyaniline (5.46 g, 0.05 mol) was dissolved in dilute hydrochloric acid (12 cm^3 37% aq. HCl + 40 cm^3 of water) and cooled to 0–3°C. To this mixture an aqueous solution of sodium nitrite (3.45 g, 0.05 mol in 18 cm^3 of water) was slowly added dropwise under continues stirring. Next the obtained diazonium salt was diluted with 200 cm^3 of precooled ethanol. Separately phenol (4.7 g, 0.05 mol) was dissolved in 42 cm^3 10% NaOH and 50 cm^3 of ethanol, and this mixture was also cooled to 0–3°C. The phenolate solution was added dropwise under stirring to the diazonium salt and the dark-red solution was obtained. Azo coupling was continued for 4 h in 5°C, and then the solution was neutralized with dilute hydrochloric acid. The yielded red solid was filtered, washed with water and dried. The crude material was recrystallised from methanol to give 5.2 g (49%) dark-red solid of mp 215–216°C.

^{1}H-NMR (acetone-d$_6$), δ (ppm); 8.9 (2H, s, OH), 7.85 (4H, d, $J =$ 9.0 Hz, arom.), 6.95 (4H, d, $J = 9.0$ Hz, arom.).

FTIR (KBr), ν (cm^{-1}); 3458–3193 (-OH), 3017, 1608–1591, 1507–1430, 844 (arom.), 1251–1105 (C-O).

4.1.2. Esterification

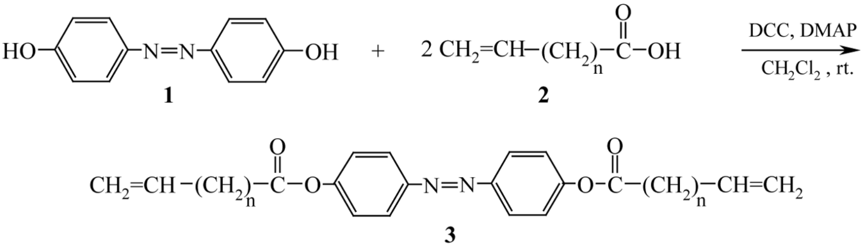

n=2 (**3a**) or 8 (**3b**)

To 0.1 mol of mesogenic diol **1** (2.14 g) and 0.02 mol of 4-pentenoic acid **2a** (2.00 g) or 10-undecenoic acid **2b** (3.76) in 80 cm^3 of dry dichloromethane, 0.022 mol (4.54 g) of N,N-dicyclohexylcarbodiimide

(DCC), and a catalytic amount ($8 \cdot 10^{-4}$ mol, 0.0977 g) of 4-dimethylaminopyridine (DMAP) were added. The reaction mixture was stirred for 24 h, then N,N-dicyclohexylurea (DHU) was filtered off and, after removal of the solvent, crude products were crystallised from methanol. Yields 52% of **3a**, 47.5% of **3b**.

3a: ^{1}H-NMR ($CDCl_3$), δ (ppm); 7.9 (4H, d, $J = 8.9$ Hz, arom.), 7.2 (4H, d, $J = 9.0$ Hz, arom.), 5.85 (2H, m, CH=), 5.1 (4H, m, $=CH_2$), 2.55 (8H, m, $-(CH_2)_2-$).

FTIR (KBr), ν (cm^{-1}); 3082, 1600–1495, 861 (arom.), 2999–2856 (CH_2), 1744 (C=O), 1643, 916 ($C{=}C_{aliph.}$), 1234–1095 (C-O).

3b: ^{1}H-NMR ($CDCl_3$), δ (ppm); 7.9 (4H, d, $J = 8.8$ Hz, arom.), 7.2 (4H, d, $J = 8.9$ Hz, arom.), 5.75 (2H, m, CH=), 4.95 (4H, m, $=CH_2$), 2.55 (4H, m, $-CH_2-$), 2.15 (4H, m, $-CH_2-$), 1.8 (4H, m, $-CH_2-$), 1.45 (20H, m, $-(CH_2)_5-$).

FTIR (KBr), ν (cm^{-1}); 3079, 1589–1470, 858 (arom.), 2923–2851 (CH_2), 1747 (C=O), 1641, 914 ($C{=}C_{aliph.}$), 1245–1097 (C-O).

4.1.3. Epoxidation

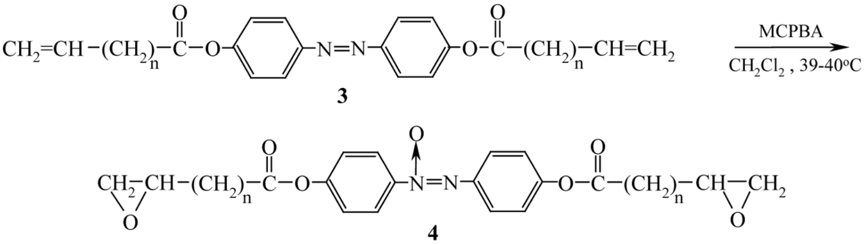

n=2 (**4a**) or 8 (**4b**)

Under continuous stirring, 8.13 g (0.033 mol, 70%) of m-chloroperoxybenzoic acid (MCPBA) was added to a solution of 0.01 mol of diolefin (3.78 g of **3a** or 5,46 g of **3b**) in 80 cm^3 of dichloromethane. The mixture was refluxed for 48 h (the reaction was monitored by TLC). After cooling and subsequent filtration, the mixture was washed with 100 cm^3 of aqueous 5% Na_2SO_3, 100 cm^3 of aqueous 5% $NaHCO_3$, 40 cm^3 of aqueous 30% NaCl. The dichloromethane layer was dried over $MgSO_4$ and evaporated. Recrystallization from methanol yielded the final products: 73% of **4a**, epoxy number (EN) = 0.465 (calcd. 0.469), and 78% of **4b** EN = 0.334 (calcd. 0.337).

4a: ^{1}H NMR ($CDCl_3$), δ (ppm); 8.25 (4H, m, arom.), 7.2 (4H, m, arom.), 3.0 (2H, m, CH of epoxy), 2.75 (4H, m, CH_2 of epoxy), 2.55 (4H, m, $-CH_2-$), 1.9 (4H, m, $-CH_2-$).

FTIR (KBr), ν (cm^{-1}); 3114–3057, 1610–1469, 860 (arom.), 2991–2928 (CH_2), 1752 (C=O), 1410, 1307–1293 ($N \rightarrow O$), 1222–1102 (C-O), 914, 841 (epoxide).

4b: ^{1}H NMR ($CDCl_3$), δ (ppm); 8.25 (4H, m, arom.), 7.2 (4H, m, arom.), 2.95 (2H, m, CH of epoxy), 2.75 (2H, m, CH_2 of epoxy), 2.55 (4H, m, -CH_2-), 2.45 (2H, m, CH_2 of epoxy), 1.8 (4H, m, -CH_2-), 1.4 (24H, m, -$(CH_2)_6$-).

FTIR (KBr), ν (cm^{-1}), 3055, 1610–1466, 859 (arom.), 2924–2850 (CH_2), 1759 (C=O), 1414, 1318–1293 (N→O), 1200–1105 (C-O), 912, 843 (epoxide).

4.2. Physical Properties

Phase transitions in the investigated materials were analyzed using DSC, polarizing microscope, and dielectric measurements. Example DSC diagrams for compound **4b** are shown in Fig. 2 (for both heating and cooling). The phase transitions solid/mesophase and mesophase/isotropic liquid are clearly seen, but there are also small peaks between the two main transitions, which suggest existence of two different mesophases (having similar molecular arrangement). In the material **4a**, only one mesophase is observed.

The optical microscopy observations (Fig. 3) enabled identification of the DSC peaks with solid–liquid crystal phase transitions. The investigated materials were placed between plates covered with ordering layers (enforcing a homogenous planar orientation, Fig. 3a).

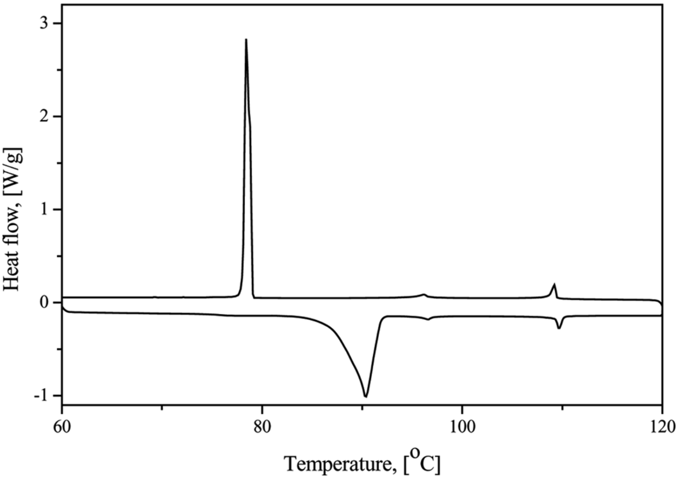

FIGURE 2 Example of an exothermic DSC thermogram of compound **4b**, recorded at heating and cooling rate of 2°C/min. Visible peaks correspond to phase transitions detected. See Table 1 for details.

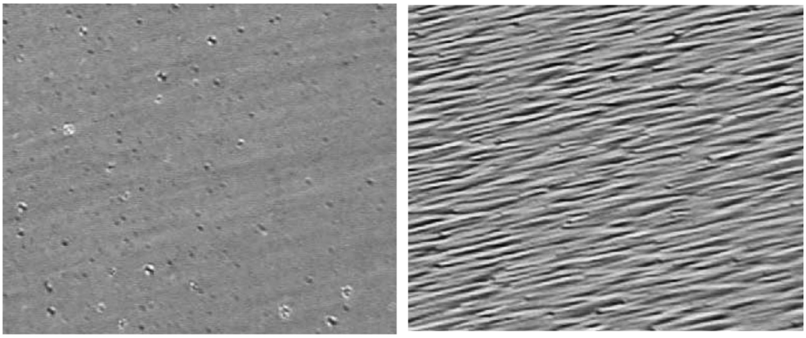

(a) (b)

FIGURE 3 Textures of the investigated compounds, observed in a polarizing microscope between crossed polaroids. Sample placed between glass plates covered with rubbed polyimide layers, enforcing planar orientation of the molecules: (a) nematic phase of compound **4b**, T = 98°C; (b) changes in the texture, smectic A phase in compound **4b**, T = 90°C.

The microscopic observations in liquid crystal cell with parallel rubbing suggest the existence of a nematic mesophase below 110°C in both compounds (the images are almost the same and look like the one shown in Fig. 3a), and compound **4a** retains a similar texture up to temperatures slightly exceeding 140°C. In the case of compound **4b**, a noticeable change occurs in the microscopic image of the sample during cooling below 97°C, which remains stable in the further course of the cooling (Fig. 3b). We can conclude from this observation that a smectic phase appears in cooling. In the course of the heating, some changes are also visible in the sample, but they are not distinctive enough to allow for clear conclusion whether or not a smectic–nematic transition exists here. The microscopic observations in the cell without rubbing show a homeotropic texture for both compounds. In this case, there are no visible changes between the two mesophases of compound **4b** during cooling, i.e., the smectic phase also has a homeotropic texture. Smectic A phases have been found to be optically uniaxial and frequently show such textures [17]. Smectic type C, where molecules are tilted within the layers, cannot have this texture [18–21]. It could appear in smectic type B, but high degree of molecular alignment within the layers in that phase would result in much stronger DSC peak for smectic–nematic transition than the one observed in our case.

The existence of two mesophases in compound **4b** was confirmed by dielectric observations. The results for both compounds are shown in Fig. 4. The static dielectric permittivity depends on the phase of the

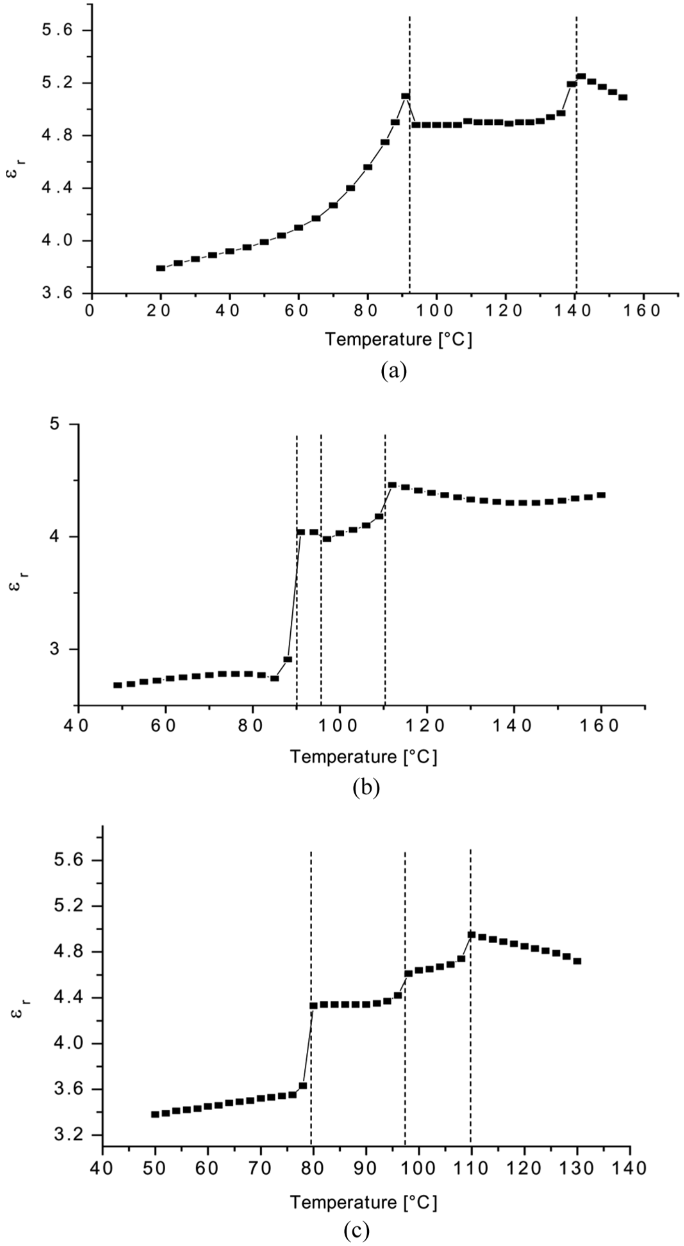

(a)

(b)

(c)

FIGURE 4 Changes in the dielectric constant corresponding to phase transitions in the materials: (a) cooling of compound **4a**; (b) heating; and (c) cooling of compound **4b**.

material because of changing in mean orientation of molecular dipoles (or induced dipoles in non-polar molecules). During the phase transition from isotropic liquid to liquid crystal, the dielectric permittivity can increase or decrease depending on the alignment in the sample (and the direction of dipole moment of the molecule), and during crystallization the dielectric permittivity mostly decreases. So the self-ordering in mesophase causes that the phase transition is observed in dielectric measurements in almost all liquid crystals. In the case of compound **4b**, the phase transition between the mesophases is also clearly seen (Fig. 4b,c) because of different arrangement of molecules in the smectic phase (layer formation affects the molecular interactions). The summarized results of measurements are presented in Table 1.

The above conclusions were confirmed by WAXS measurements performed for samples in thin capillaries. In temperatures below 110°C similar patterns were obtained for both compounds (Fig. 5a). The diffraction images show two pairs of crescent-shaped, diffuse reflections positioned at different scattering angles. This type of pattern is typical for nematics [22]. The lack of any other diffraction maxima and strong diffusion of the reflections (for both wide and small angles) indicates that there is no higher-level ordering. The diffraction pattern changes noticeably for compound **4b** after cooling below 97°C (Figs. 5b, 6). The basic feature of the image (two pairs of reflections) remains visible, but in the lower temperature the intensity of the small-angle reflections is much larger, which indicates stronger correlation in molecular arrangement along the mean direction of their axes (a different mesophase) and is therefore in accordance with optical observations. Below 80°C, the pattern is typical for solid state (Fig. 6).

Images similar to those acquired in temperatures below 110°C have been obtained by other authors (*e.g.*, [19]) for different nematic materials. The appearance of arcs rather than rings reflects orientation of the sample, induced by interaction between the molecules and the

TABLE 1 Phase Transitions in the Investigated Compounds, According to DSC, Dielectric, and Optical Analysis

Materials	Temperatures of phase transitions [°C]	Comments
First	Cr 105 N 143 I	heating
compound (**4a**)	Cr 93 N 141 I	cooling
Second	Cr 90 SmA 97 N 110.5 I	heating
compound (**4b**)	Cr 80 SmA 97 N 110 I	cooling

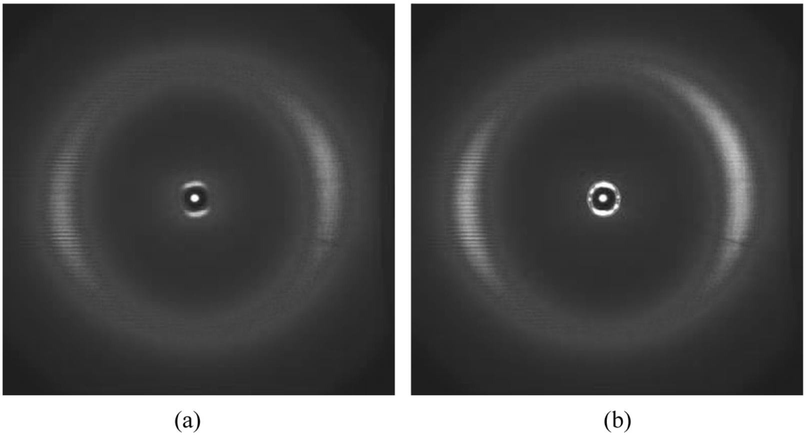
(a) (b)

FIGURE 5 Examples of WAXS 2D patterns: (a) material **4b**, T = 103°C; the diffraction pattern (two diffuse rings) is typical for nematics; (b) material **4b**, T = 87°C; the diffraction pattern (two rings, sharp small-angle ring) is typical for smectics A.

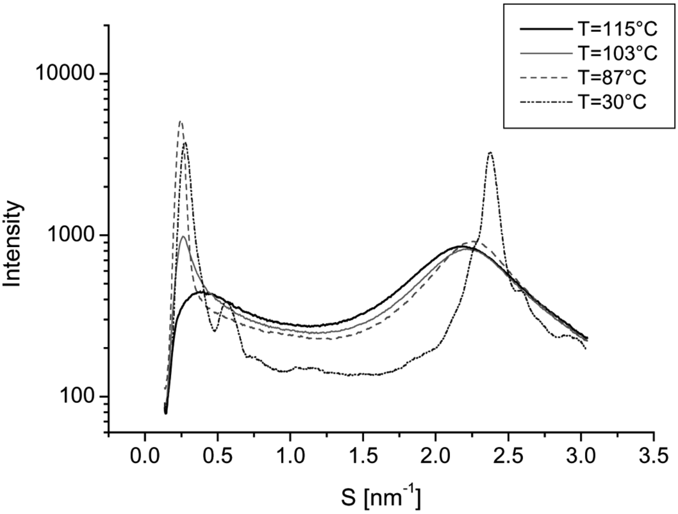

FIGURE 6 The plot of X-ray scattering intensity *vs*. scattering vector *s* for material **4b**. Two diffraction maxima are visible in the isotropic and nematic phase; the peaks at small values of *s* are much stronger and narrower in smectic A phase; a different pattern can be observed in the solid state.

capillary walls. The director **n** of the structure is perpendicular to the imaginary line connecting the centres of both wide-angle arcs [23,24].

Formation of smectic layers creates positional correlation in the system, which gives rise to diffraction maxima at small angles. As the smectic phase is approached on cooling from the nematic phase the diffuse spots in the nematic structure factor sharpen and eventually become the quasi-Bragg peaks of the smectic phase [22]. We can see similar behavior in our case, where below 97°C the intensity of the small angle peaks for compound **4b** becomes much stronger (Fig. 6). The wide-angle diffraction pattern exhibits two crescent-shaped maxima in equatorial positions, similar to those observed in the nematic phase, which means that there is no two-dimensional lattice formation inside the layers (Figs. 5, 6). In liquid-like layers of both smectics A and C, a diffuse ring was also observed by other authors [22,24]. However, the pairs of wide-angle and small-angle reflections in smectics C are not perpendicular to each other, as in the case of smectics A (and our samples). WAXS results are therefore consistent with other results indicating formation of smectic A phase in our case.

Considering the scattered intensity as a function of the scattering vector **s** ($s = 2\sin\theta/\lambda$, where θ is the scattering angle and λ is the wavelength [22]) it is possible to obtain the approximate values of several parameters of the measured system. The repeat distance l corresponding to s_m (the value of scattering vector s at a diffraction maximum) may be computed as $l = 1/s_m$ [24]. This value, computed for small-angle peaks, may be directly interpreted as the approximate length of a molecule in nematics and as the layer width in smectics. The position s_m of wide-angle reflections is related to intermolecular distance d, but this relation depends on the three-dimensional geometry of the system. For ordered nematics (as well as for smectics A and C), the geometry of random packing of parallel cylinders seems to be appropriate, which results in the formula $d = 1.12/s_m$ [23,24].

The experimental results from WAXS measurements (the values of the scattering vector s_m corresponding to the diffraction peaks and the calculated structural parameters) are presented in Table 2 and compared to the lengths of the molecules obtained by *ab initio* methods, for the most extended conformers of the molecules.

The experimental values are close to those obtained from quantum mechanical calculations. The observed differences for the nematic phase are less than 10% of the calculated values. The simplest explanation of this difference is that the long axes of the molecules in nematics are not aligned strictly with the global director **n**. Instead, they may be tilted by some angle β from the direction of **n**. We can then identify the correlation length s_m^{-1} obtained from WAXS

TABLE 2 Molecular Lengths (l)* and Average Intermolecular Distances (d)* Calculated from the Positions of WAXS Maxima (s_m). For Comparison, the Molecular Lengths Obtained from *ab initio* Calculations (l_c) are also Presented

	WAXS – wide angle		WAXS – small angle		Ab initio	
Molecule	s_m [nm^{-1}]	d [nm]	s_m [nm^{-1}]	l [nm]	l_c [nm]	l/l_c
(**4a**) nematic	2.21	0.51	0.45	2.22	2.33	0.95
(**4b**) nematic	2.25	0.50	0.26	3.85	3.90	0.98
smectic A	2.30	0.49	0.245	4.08		1.05

*Values of l are computed as $l = 1/s_m$; values of d are computed as $d = 1.12\,s_m^{-1}$ assuming the model of random packing of cylinders for both the nematic and smectic A phases.

measurements with the mean projection l_n of molecular length l along the director. For the average value of $\beta \sim 30°$, which is quite reasonable for nematics, this model gives $l_n \sim 0.9\ l$ [24], which is very close to our results. It is noteworthy that at higher temperatures non-all-trans conformations also exist, which may lead to smaller values of measured layer width. There are also other factors which may influence the results. The diffraction peaks are not very sharp, which makes it difficult to determine the maximum accurately. The *ab initio* calculations were carried out *in vacuo*, without taking into consideration any intermolecular interactions. Taking all of this into account, we may conclude that the results are in good accordance with theoretical data. The value obtained for the smectic A phase (compound **4b**) is slightly larger than for the nematic phase and close to the calculated length of the molecule. This is an additional argument that smectic A is formed, as molecules do not appear to be tilted within the layers.

Another quantity obtained from WAXS results (Table 2) is the nearest neighbour distance, which is little above 0.5 nm for all the molecules considered. Similar values were found for a wide variety of compounds [24].

5. CONCLUSIONS

- A two-stage method of synthesis of diepoxy compounds has been used to obtain two new compounds. A mesophase was observed in both cases. The temperatures of phase transitions were determined with DSC, polarising microscope, and dielectric spectroscopy. The mesophase types were verified by means of WAXS technique.

- The compound **4a** has a nematic phase in wide range of temperatures (100°C–140°C) in both heating and cooling.
- The compound **4b** is isotropic liquid above 110°C and its range of mesophase is narrower. Except the nematic phase, a smectic A phase was also observed in this case, which appears in a narrow temperature range (90°C–97°C) during heating and in a wider range (97°C–80°C) during cooling.
- As we expected, connecting the same mesogen with longer carbon chains resulted in a lower temperature of the transition to isotropic phase. Extending the chains also led to the appearance of a second, smectic mesophase, but at a cost of much smaller range of the nematic phase.
- Lengths of the molecules obtained experimentally from WAXS results are in agreement with those obtained in quantum mechanical calculations (RHF method with 6–31G* basis set).

6. ACKNOWLEDGMENTS

Part of this work was supported by the Polish Committee of Scientific Research (KBN), grant N205 060 31/2543.

REFERENCES

[1] Naemura, S. (2001). *Displays*, *22*, 1.

[2] Demeter, G. & Krimer, D. O. (2007). *Phys. Reports*, *448*(5–6), 133.

[3] Hwang, S. H., Lim, Y. J., Lee, M.-H., Lee, S. H., Lee, G.-D., Kang, H., Kim, K. J., & Choi, H. C. (2007). *Curr. Appl. Phys.*, *7*(6), 690.

[4] Brown, D. H., Das, V., Allen, R. W. K., & Styring, P. (2007). *Mater. Chem. and Phys.*, *104*(2–3), 488.

[5] Chung, T.-S. (Ed.) (2001). *Thermotropic Liquid Crystal Polymers: Thin-Film Polymerization, Characterization, Blends, and Applications*, Technomic Publising Company, Inc.: Lancaster, PA.

[6] Kelar, K. & Ciesielska, D. (1997). *Fizykochemia polimerów – Wybrane zagadnienia* (in Polish). Wydawnictwo Politechniki Poznańskiej: Poznan.

[7] Carfagna, C., Amendola, E., & Giamberini, M. (1997). *Prog. Polym. Sci*, *22*, 1607.

[8] Rozenberg, B. A. & Gur'eva, L. L. (1992). Oriented liquid crystalline network polymers. In: *Synthesis, Characterization and Theory of Polymeric Networks and Gels*, Aharony, S. M. (Ed.), Plenum Press: New York, 147–164.

[9] Kurihara, S., Sakamoto, A., & Nonaka, T. (1998). *Macromol.*, *31*(14), 4648.

[10] Włodarska, M., Bąk, G., Mossety-Leszczak, B., Galina, H., & Pakuła, T. (2007). *J. Non-Cryst. Solids*, *353*, 4371.

[11] Frisch, M. J. *et al.* (1998). *Gaussian 98*, Gaussian, Inc.: Pittsburgh, PA.

[12] Wlodarska, M., Bąk, G., & Bartczak, W. (2002). *J. Mol. Struct. (Theochem)*, *619*, 59.

[13] Kuze, N., Ebizuka, M., Fujiwara, H., Takeuchi, H., Egawa, T., & Konaka, S. (1998). *J. Phys. Chem. A*, *102*, 2080.

[14] Schlegel, H. B. (1982). *J. Comp. Chem.*, *3*, 214.

[15] Vanoppen, P., Grim, P. C. M., Rücker, M., de Feyter, S., Moessner, G., Valiyaveettil, S., Müllen, K., & de Schryver, F. C. (1996). *J. Phys. Chem.*, *100*, 19636.

[16] Ruslim, Ch., & Ichimura, K. (1999). *J. Mater. Chem.*, *9*, 673.

[17] de Vries, A. (1979). Structure and classification of thermotropic liquid crystals. In: *Liquid Crystals*, Saeva, F. D. (Ed.), Marcel Dekker, Inc., New York/Basel, 1.

[18] Doucet, J. (1979). X-ray studies of ordered smectic phases. In: *The Molecular Physics of Liquid Crystals*, Luckhurst, G. R., & Gray, G. W. (Eds.), Academic Press: London, 317.

[19] Petrie, S. E. B. (1979). Smectic liquid crystals. In: *Liquid Crystals*, Saeva, F. D. (Ed.), Marcel Dekker, Inc., New York/Basel, 163.

[20] Donald, A. M. & Windle, A. H. (1992). *Liquid Crystalline Polymers*, Cambridge University Press: Cambridge.

[21] de Gennes, P. G. & Prost, J. (1993). *The Physics of Liquid Crystals*, 2nd ed., Clarendon Press: Oxford.

[22] Vickers, M. E. (1995). Wide angle x-ray scattering. In: *Scattering Methods in Polymer Science*, Richards, R. W. (Ed.), Ellis Horwood: London, 103–152.

[23] de Vries, A. (1970). *Mol. Cryst. Liq. Cryst.*, *10*, 219.

[24] Leadbetter, A. J. (1979). Structural studies of nematic, smectic A and Smectic C phases. In: *The Molecular Physics of Liquid Crystals*, Luckhurst, G. R., Gray, G. W. (Eds.), Academic Press: London, 285–316.